Shear and Bending Properties of Homogeneous and Hybrid CLT Panels Fabricated from Low-Value North American Hardwood Species

Balazs Bencsik Levente Denes Eduardo M. Sosa
Curt C. Hassler Joseph F. McNeel

Abstract

This study examines the mechanical properties of the homogeneous and hybrid lay-up cross-laminated timber (CLT) made from red oak, red maple, and yellow poplar. The selection of species was based on the availability of less marketable natural resources in the Appalachian region. This region is known for its diverse and abundant hardwood forests featuring dominant species like white and red oaks, yellow poplar, soft maples, hickory, and beech. Demonstrating the suitability of the selected species for structural purposes can open new pathways for developing new, valuable engineered wood products and can expand the raw material resources. For the three-layer CLT manufacturing phenol-resorcinol-formaldehyde and polyurethane adhesives were used. A variable-span regression model was used to assess the effective bending stiffness and shear properties of CLT panels. The results showed that the span-to-depth ratio significantly affects the effective and apparent bending modulus ratios and varies slightly by lay-up configuration. A strong linear correlation ($r^2 = 0.735$) was found between the apparent and effective modulus of elasticity, allowing the prediction of effective modulus from apparent values. The effect of the applied adhesive was insignificant on the performances tested. The lay-up configuration significantly affected the shear strength performance. Although hybrid CLTs had approximately 30 percent lower shear strength than homogeneous ones, their performance still exceeded softwood CLTs, with shear strengths ranging from 2.38 N/mm^2 to 2.52 N/mm^2. On average, the shear analogy model underestimated the effective bending stiffness by 8.9 percent and the shear stiffness by 74.8 percent across different CLT configurations. The numerical simulation results for the stiffness properties of each CLT panel type show a reasonable agreement with the experimental test data. These findings highlight the potential of hardwood CLT to improve structural performance, especially in bending, although shear limitations in hybrid configurations should be considered.

The beneficial mechanical, installation, and sustainability properties of cross-laminated timber (CLT) panels position them as real alternative of the conventional construction materials. Just as with the emergence of mass-produced steel beams, architects now aim to design the tallest possible buildings using mass timber products, bringing the glulam and CLT into the spotlight.

The authors are, respectively, *a*, Title, Post-doctoral Fellow School of Natural Resources and the Environment, Davis College of Agriculture and Natural Resources, West Virginia University Morgantown, West Virginia, and Post-doctoral Fellow, Appalachian Hardwood Center, West Virginia University, Morgantown, West Virginia (balazs.bencsik@mail.wvu.edu[corresponding author]; Title, Associate Professor School of Natural Resources and the Environment, Davis College of Agriculture and Natural Resources, West Virginia University Morgantown, West Virginia (ldenes@mail.wvu.edu); Title, Associate Research Professor Department of Mechanical, Materials, and Aerospace Engineering, West Virginia University, Morgantown, West Virginia (eduardo.sosa@mail.wvu.edu); Title, Research Professor Appalachian Hardwood Center, West Virginia University, Morgantown, West Virginia (chasslerwv@gmail.com); and Title Professor, School of Natural Resources and the Environment, Davis College of Agriculture and Natural Resources, West Virginia University Morgantown, West Virginia, and Title, Director Appalachian Hardwood Center, West Virginia University, Morgantown, West Virginia (jmcneel@wvu.edu). This paper was received for publication in March 2025. Article no. 25-00011.

Forest Prod. J. 75(4):319–331.
doi:10.13073/FPJ-D-25-00011

Depending on the mechanical requirements of a certain panel in the building structure, CLT can be adjusted based on the properties of the raw material, the lay-up configuration, and the panel thickness. In North America, the design properties of CLT based on grades and lay-ups are listed in the ANSI/PRG 320 (APA 2019) standard. Currently, softwood species such as spruce-pine-fir, Douglas-fir-larch, southern pine, hem-fir, and engineered wood products such as laminated veneer lumber (LVL) and oriented strand board (OSB) are allowed for use in CLT manufacturing.

Like all structural materials, CLT has its weaknesses, which must be considered during engineering design. The cross-layered arrangement of the boards can weaken the structure by making the cross layers prone to rolling shear failure when subjected to out-of-plane loading with short-spans or openings (Aicher et al. 2016, Ehrhart and Brandner 2018). In short-span bending, the rolling shear stiffness and strength properties of the lamellae in the transverse layers play a key role in controlling the load-bearing capacity of CLT beams. Typically, the failure of a CLT beam begins with rolling shear in the transverse layers, followed by tension failure in the longitudinal outer layers, which indicates that CLT has complex failure mechanisms (Brandner et al. 2016). Consequently, in addition to bending stiffness (EI_{eff}) and bending moment ($[F_bS]_{eff}$), predicting shear stiffness (GA_{eff}) and shear capacity (V_s) are always two essential properties in the structural characterization of CLTs. The North American ANSI/PRG 320 (APA 2019) standard refers to determining the shear characteristics of CLT using the ASTM D198 (ASTM 2015) standard method with short-span bending. Another approach is provided by the ASTM D2718 (ASTM 2018) standard, commonly known as the planar shear test. Based on this test, several modified versions, referred to as Modified Planar Shear (MPS) tests, have been proposed and used in numerous studies (Nero et al. 2022, Wang et al. 2017, Wang et al. 2024). Both test methods can yield comparable rolling strength properties (Li 2017). Alongside the mechanical test methods, four analytical models—the Gamma method (Sandoli and Calderoni 2020), k-method (Schultz 2017), Shear Analogy (Adhikari et al. 2023), and Timoshenko Beam Theory (Rahman et al. 2020a)—are used to determine the design mechanical properties of CLT. The accuracy of these models varies depending on the lay-up configuration of the CLT, the wood species used, the length-to-depth ratio, and the variation in shear modulus between layers—all of which significantly influence shear performance and deflection predictions. (Rahman et al. 2020b, Huang et al. 2023).

Several studies have shown that the shear rigidity and rolling shear strength of engineered wood products are based not only on material properties but also on apparent system properties. Based on these findings, there are two main approaches to improve the CLT's shear performance. The first is to manufacture CLT using wood species with higher shear strength and stiffness. Hardwood species, which generally have superior shear performance perpendicular to the grain compared to softwoods, offer a promising solution for the transverse layers of CLT. A considerable number of studies have confirmed that the rolling shear strength ranges from 1.0 MPa to 2.0 MPa, and the average shear modulus is typically about 100 MPa for most of the CLTs made from softwood species (Bendtsen, 1976, Dahl and Malo 2009, Zhou et al. 2014, Gong et al. 2015, Brandner et al. 2016, Sikora et al. 2016, He et al. 2018, Lim et al. 2020). In contrast, depending on the hardwood species, experimental hardwood CLT rolling shear strength ranges from 3.0 MPa to 5.85 MPa, and the modulus ranges from 150 MPa to 350 MPa (Aicher et al. 2016, Franke 2016, Ehrhart and Brandner 2018, Rara 2021). Two previous studies by Ma et al. comprehensively examined the mechanical properties of CLT manufactured from sugar maple and proved that even low-value variants of this species have potential for use in CLT manufacturing. (Ma et al. 2021a, Ma, et al. 2021b). Alongside its mechanical advantages, the mass production of CLT from hardwood species faces several challenges, such as dimension lumber manufacturing, effective structural grading, sufficient gluing technology, and the significantly higher price of lumber (Adhikari et al. 2020, Hassler et al. 2022).

Among hardwood species, engineered wood products such as laminated veneer lumber (LVL), plywood, oriented laminated strand lumber (LSL) or oriented standard board (OSB) offers a viable option to increase CLT's resistance to rolling shear failure (Wang et al. 2015, Brandner et al. 2016, Wang et al. 2017, Li and Ren 2022, Yang et al. 2023).

Regardless of the wood species used, optimizing the system arrangement including the lay-up orientation, sawing pattern, and width-to-thickness ratio of the lumber, presents a second opportunity to increase the shear resistance of CLT. The impact of material dimensions and anatomical characteristics on the shear performance of CLT is an intensively researched area.

Ehrhart and Brandner (Ehrhart and Brandner 2018), as well as Jakobs (Jakobs 2005), identified an optimal width-to-thickness ratio of $w\ell/t\ell = 150/30 = 5$, which exceeds the minimum ratio of 3.5 required by the ANSI/PRG 320 (APA 2019) standard. Additionally, the highest shear stiffness was observed with an annual ring orientation angle between 30° and 55° (β). This result aligns with Görlacher's findings, which identified 45° as the optimal annual ring angle (β) (Görlacher 2002).

Related to the manufacturing technology Wang et al. examined the effects of edge-gluing and gaps on the rolling shear properties of CLT made from spruce-pine-fir (Wang et al. 2018.). They reported that when the edges are connected, the glued connection does not significantly influence the shear performance. However, a gap of 2 mm or more significantly reduces the shear strength and stiffness of the specimens. One explanation is that the gaps can introduce stress riser effects, therefore decreasing ultimate shear strength (Gardner et al. 2020).

Even though deviating from the standard 90-degree orientation of transverse layers is not common practice in CLT manufacturing, Bahmanzad et al. demonstrated that altering the fiber orientation can significantly enhance shear performance (Bahmanzad et al. 2020). They reported that in CLT made from eastern hemlock, the shear strength of cross layers with 30° and 45° fiber orientations relative to the major panel axis was 98 percent and 59 percent greater, respectively, than those of layers with a 90° orientation.

This study aimed to evaluate the bending and shear properties of homogeneous and hybrid CLT panels, manufactured exclusively from lower-grade North American hardwood species and two widely used adhesive types. The CLT panels were produced from 25 mm (1 inch) thick, low-grade red oak, red maple, and yellow poplar lumber in three-layer configurations with various lay-up designs. For gluing, 1-component polyurethane and phenol-resorcinol-formaldehyde adhesives were used. A variable-span regression model was employed to

assess the effective bending stiffness and shear properties of the CLT. The experimental results were then compared with the predicted values obtained from the shear analogy method. A combination of orthotropic material properties reported in the literature and shear modulus values obtained from the regression methods were adopted for the finite element (FE) method to determine the elastic response of the CLT panels subjected to center-point bending.

Materials and Methods

Lumber preparation and panel manufacturing

CLT testing specimens were manufactured from 25 mm thick, 178 mm wide, and 3.1 m long surfaced lumber made from yellow poplar (*Liriodendron tulipifera*), red oak (*Quercus rubra*), and red maple (*Acer rubrum*) hardwood species were acquired from the northeast West Virginia Appalachian region. All boards were graded as No. 2B and No. 3B Common according to the National Hardwood Lumber Association (NHLA 2014) grading rules. All lumber was also subjected to visual strength regrading based on the "Standard Grading Rules for Northeastern Lumber" published by the Northeastern Lumber Manufacturers Association (NELMA 2024.) to select the longitudinal and transverse layers of the CLT panel. For the longitudinal layers, No. 2 graded lumber was selected, although No. 3 graded lumber was used for the transverse layers. The visually strength-graded lumber was conditioned for three months in the conditioning room to achieve a uniform moisture content of 12 ± 1 percent. After conditioning, the dynamic modulus of elasticity (MOE_d) was measured in flatwise orientation using a transverse vibration equipment (Metriguard Model 340 Transverse Vibration E-Computer). The average properties of the laminae are given in Table 1.

Before manufacturing the three-layer CLT panels, the lumber was surfaced on all four sides to a net dimension of 19 mm × 153 mm (T×W, thickness and width, respectively). For CLT fabrication, 1-component polyurethane (1C-PUR) (Henkel LOCTITE HB X602 PURBOND) with its corresponding primer (LOCTITE PR 3105 PURBOND), and phenol-resorcinol formaldehyde (PRF) (Dynea Aerodux 185+Hardener HRP.150) adhesives were used. In total, eight 57 mm thick, 915 mm wide, and 3,050 mm long panels were manufactured. Table 2 shows the eight panel configurations and the manufacturing parameters. Each type of CLT panel was cut into three beams, each measuring 300 mm wide and 1,722 mm long, which were then subjected to bending tests. The beams were subsequently shortened from 1,722 mm to 1,257 mm, then to 869 mm, then to 586 mm, and finally to 297 mm, according to the specific span-to-depth ratios described in the static bending test method section. The length reduction was applied symmetrically at both ends of the specimens. In all cases of the hybrid configurations, the yellow poplar laminates were used in the middle (transverse) layer.

Table 1.—Density and dynamic flexural properties of the laminae.

	Species				
	Red maple		Red oak		Yellow poplar
Properties	No. 2 grade	No. 3 grade	No. 2 grade	No. 3 grade	No. 3 grade
Avg. density (kg/m^3)	617	605	692	710	486
$CoV_{density}$ (%)	5.2	6.4	6.1	7	9.3
Avg. MOE_d (GPa)	11.98	12.27	13.14	13.07	12.76
CoV_{MOEd} (%)	9.9	8.7	10.6	9.8	10.3

Measurement of bending and shear properties of CLT panels using the multiple regression method according to the ASTM D198 procedures

Using the apparent modulus of elasticity (E_{app}) values from the variable span bending tests on a timber beam, the shear modulus (G) and the effective modulus of elasticity (E_{eff}) can be obtained through linear regression analysis. Although the CLT has an orthotropic composite structure, the method can measure only the global effective shear modulus (G_{eff}). The elastic deflection of a prismatic shear modulus specimen under a single-center point load is:

$$\Delta = \frac{Pl^3}{48EI_{app}} = \frac{Pl^3}{48EI_{eff}} + \frac{Pl}{4\kappa GA_{eff}} \quad (1)$$

where EI_{app} (N-mm^2/m of width) is the apparent bending stiffness, EI_{eff} (N-mm^2/m of width) is the effective bending stiffness, GA_{eff} (N/m of width) is effective shear stiffness, P is the concentrated load applied at midspan, l is the span (mm), and κ is the shear coefficient equal to 5/6 for a rectangular section.

Removing like terms and solving for the inverse apparent bending stiffness and inverse effective bending stiffness produces Eq. 2:

$$\frac{1}{EI_{app}} = \frac{1}{EI_{eff}} + \frac{1}{GA_{eff}}\left(\frac{12}{\kappa l^2}\right) \quad (2)$$

Eq. 2. can be expressed as a linear function by substituting $y = 1/EI_{app}$ and $x = 12/\kappa l^2$ equations of a line, $y = mx + b$. The slope of the line is the reciprocal of the effective shear stiffness (GA_{eff}), and y-intercept is the reciprocal of the effective bending stiffness (EI_{eff}), which is illustrated in Figure 1.

When a single-center point load is applied, the apparent modulus of elasticity can be computed using the following:

$$MOE_{app,c} = \frac{Pl^3}{48I\Delta} \quad (3)$$

By applying a four-point bending condition, the apparent modulus of elasticity can be computed using the following formula:

$$MOE_{app,f} = \frac{23Pl^3}{108bd^3\Delta} \quad (4)$$

where P and Δ correspond to the load/deflection (N/mm) pair in elastic zone, l is the length of the span (mm) and I is the moment of inertia (mm^4).

The overall effective shear modulus (G_{eff}) of the panel can be expressed as

$$G_{eff} = G_{eff}/A \quad (5)$$

where A is the gross cross-sectional area subjected to shear forces (mm^2).

Table 2.—CLT panel configurations and manufacturing parameters.

Type of CLT	Adhesive type	Adhesive spread rate (g/m^2)	Primer spread rate (g/m^2)	Clamping pressure (N/mm^2)	Pressing time (min)
Homogenous red maple (HRM-PRF)	PRF	250	N/A	0.7	360
Homogenous red maple (HRM-PUR)	PUR	200	20	0.7	150
Homogenous red oak (HRO-PRF)	PRF	250	N/A	0.7	360
Homogenous red oak (HRO-PUR)	PUR	200	20	0.7	150
Maple-Y. poplar hybrid (RMYP-PRF)	PRF	250	N/A	0.7	360
Maple-Y. poplar hybrid (RMYP-PUR)	PUR	200	20	0.7	150
Oak-Y. poplar (ROYP-PRF)	PRF	250	N/A	0.7	360
Oak-Y. poplar (ROYP-PUR)	PUR	200	20	0.7	150

Due to the orthogonal structure of CLT, the shear strength is not evenly distributed among the layers. The equivalent shear strength can be calculated as (Ma et al. 2021b):

$$f_{s,eq} = \frac{P_{max}}{2 \cdot A} \tag{6}$$

where P_{max} is the peak of the force, A is the gross cross-sectional area subjected to shear forces (mm^2).

Prediction of stiffness properties of CLT based on Shear Analogy method

The method has been adopted by the ANSI/PRG 320 (APA 2019) product standard, which provides the most precise analytical design values for CLT (Karacabeyli and Gagnon 2019). The value of EI_{eff} for the shear analogy method is predicted as

$$EI_{eff} = \sum_{i=1}^{n} E_i b_i \frac{h_i^3}{12} + \sum_{i=1}^{n} E_i b_i h_i z_i^2 \tag{7}$$

where E_i is the modulus of elasticity of the laminate in the ith layer (MPa), b_i is the CLT width in the CLT major strength direction (mm), h_i is the thickness of laminate in the ith layer, z_i is the distance between the center point of the ith layer and the neutral strength direction, and n is the number of layers in the CLT.

The effective shear stiffness GA$_{eff}$ for the major strength direction can be calculated as

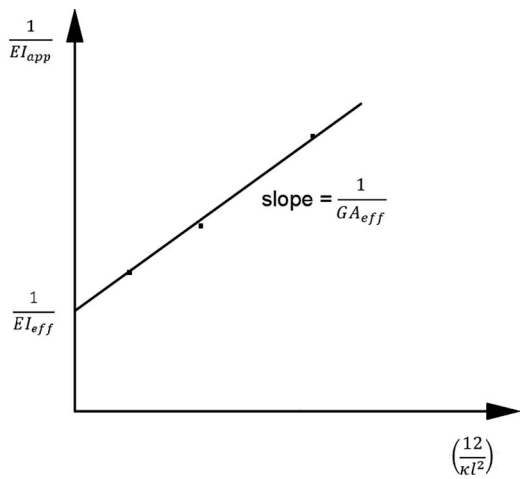

Figure 1.—Schematic representation for determination of effective shear stiffness and effective bending stiffness.

$$GA_{eff} = \frac{a^2}{\left[\left(\frac{h_1}{2G_1 b_0}\right) + \left(\sum_{i=2}^{n-1} \frac{h_i}{G_i b_0}\right) + \left(\frac{h_n}{2G_n b_0}\right)\right]} \tag{8}$$

where

$$a = \sum_{i=1}^{n} h - \frac{h_1}{2} - \frac{h_n}{2} \tag{9}$$

where

G_i is the shear modulus of the laminate in the ith layer (MPa), G_1 is the shear modulus of the first layer of CLT (MPa) G_n is the shear modulus of the laminate in the nth layer (MPa).

The dynamic modulus of elasticity (MOE$_d$) of the lumber was used to calculate the design values. Regarding the orientation of the lumber in the panel layup, MOE$_d$ was applied for the longitudinal (parallel) major direction, and MOE$_d$/30 for the perpendicular (transverse) layers. The shear stiffness (G) of the lumber in the parallel layer was assumed to be MOE$_d$/16, whereas in the perpendicular layer it was assumed to be MOE$_d$/16/10 (Cherry et al. 2019).

Static bending tests of CLTs

Single-center point and four-point bending tests were used to determine the apparent modulus of elasticity (MOE$_{app}$) and the shear strength (f$_s$) in the major direction of the CLT according to ASTM D198 (ASTM 2015). The load direction for each method was flatwise and four different span-to-depth ratios were applied. The testing details of the four beam lengths are shown in Table 3.

Three span-to-depth ratios (22:1, 15:1, 10:1) were applied to determine the MOE$_{app}$ for the regression model, and in the case of the last setup (5:1 span-depth ratio) the test was carried out until failure. After each stiffness measurement on a certain span, the specimens were cut to the shortened span plus a 6 mm overhang on each side. The overhang beyond the span was minimized, as the shear capacity may be influenced

Table 3.—Bending test setup parameters.

Loading conditions	Span (mm)	Length-to-depth ratio (l/d)	Loading rate (mm/min)	Applied max. deflection (mm)
Third-point	1,710	30	5.0	6
Center-point	1,245	22	2.5	5
Center-point	857	15	2.1	4
Center-point	574	10	2.0	2
Center-point	285	5	1.25	break

by the length of the overhang (ASTM D198) (ASTM 2015). From each type of CLT beam, three specimens were subjected to stiffness measurements using four-point and center-point bending setups. The loading and support conditions of CLTs is shown in Figure 2.

An Instron universal testing machine with an integrated load cell (300 kN, 1% sensitivity) was used for all tests. The deflection of the neutral axis at midspan was measured using a linear voltage differential transducer (LVDT) (±51 mm, 0.25% sensitivity). To calculate the apparent modulus of elasticity (MOE_{app}), the P and Δ pairs were recorded between 20 percent and 40 percent deflection in the linear elastic zone. Figure 3 shows the experimental setup for shear test of the hybrid red oak (ROYP) CLT.

Finite element model setup

The CLT configurations and experimental setup described in the previous sections were utilized as a basis for creating a finite element (FE) model of the CLT panels subjected to center-loading, as shown in Figure 2. The FE models focused on three spans, L = 574, 857, and 1245 mm, subjected to small prescribed central displacements applied to determine the stiffness in the initial nearly linear response. The models were created with the Simulia/Abaqus simulation suite (Dassault Systemes Simulia Corp. 2023) and included the following characteristics:

(a) Parts and assembly. The CLT model had two top and bottom longitudinal panels and a series of transversal panels whose number varied depending on the span length. Figure 4(a) illustrates the configuration corresponding to L = 1245 mm.

(b) Interactions. The top and bottom longitudinal panels are linked to transverse panels via a cohesive surface interaction that simulates the presence of the structural adhesive. The center line of the top longitudinal panels is coupled to a reference point (RP) created to simulate the transversal center line of load application. These interactions are illustrated in Figure 4(b).

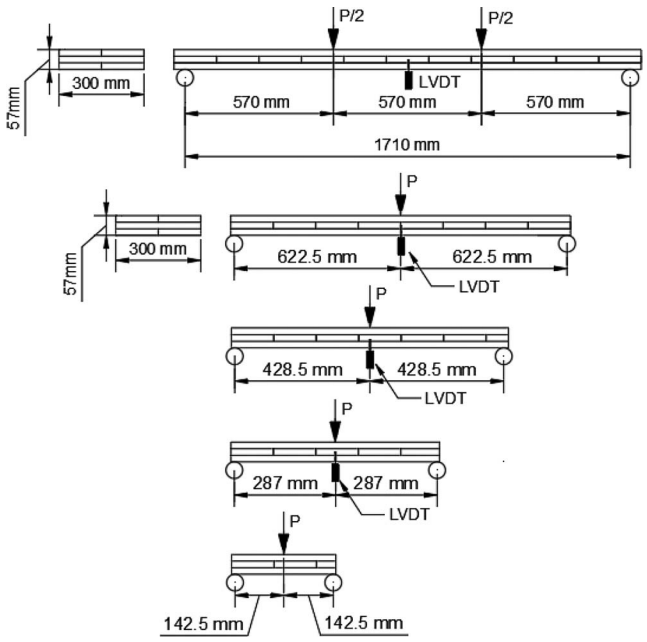

Figure 2.—Loading and support conditions of CLTs subjected to bending.

Figure 3.—Shear strength test setup of the red oak hybrid (ROYP) CLT specimen during testing.

(c) Load and boundary conditions. The CLT panel is assumed to have pinned boundary conditions on one end and roller boundary conditions on the other end. A concentrated downward displacement is applied to the RP and drives the deflection of the beam. The magnitude of the prescribed displacement varies depending on the span length, and the values adopted for the simulations are summarized in Table 3. The position of the prescribed displacement and boundary conditions are shown in Figure 4(b).

(d) Elements and mesh. All the parts are discretized using continuous three-dimensional, 8-node, linear hexahedral elements (C3D8R) with reduced integration and hourglass control. The resulting meshed configuration for a CLT beam with L = 1245 mm is shown in Figure 4(c). A control node at the center of the bottom longitudinal panel was used to monitor the deflection produced by the prescribed displacements on the different span lengths.

(e) Material properties. The layers of the CLT beam are considered orthotropic materials, and their material parameters are defined for longitudinal and transversal directions. The material orientations corresponding to each panel direction are shown in Figure 4(a). The orthotropic engineering constants corresponding to each type of wood adopted in this study were extracted from the Wood Handbook (Forest Products Laboratory, 1999) and summarized in Table 4. Note that values G_{23} for red oak and red maple are not reported in the Wood Handbook (Forest Products Laboratory, 1999). Average Geff's values, obtained from the regression analysis, were adopted instead. Moreover, the surface bonding interactions are based on the Cohesive Zone Model (CZM) available in Abaqus (Dassault Systemes Simulia Corp. 2023), in which the cohesive parameters were extracted from Tran et al. (Tran et al. 2014, Tran et al. 2015) and included the following values: Initial elastic behavior in Mode I is K_n = 4.5 MPa/mm, and for Mode II is K_t = 30 MPa/mm.

(f) Analyses. The Abaqus/Standard solution solver, including the option to capture potential geometric nonlinearities, was implemented to calculate the response of the different CLT beam configurations. The total reaction force resulting

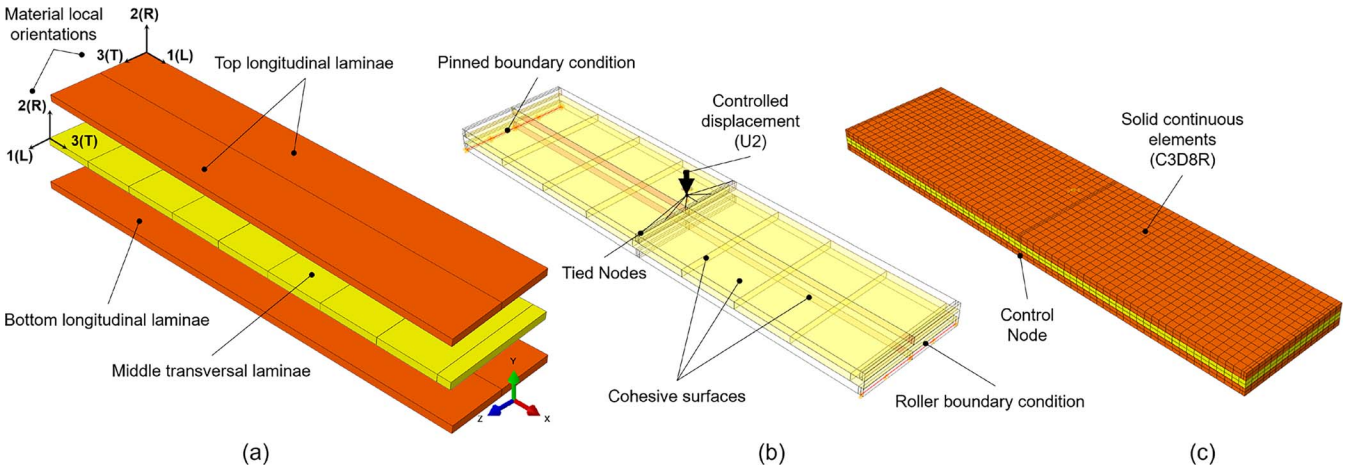

Figure 4.—Finite element model setup. (a) Parts and material orientations; (b) interactions, loading, boundary conditions; (c) meshed final configuration.

from an imposed vertical displacement applied at the RP was extracted as the primary output for the analyses.

Statistical analysis

All statistical analyses were conducted using TIBCO® Data Science/Statistica 13 software. A factorial analysis of variance (ANOVA) was performed to assess the significance of factors affecting effective bending and shear stiffness, with the significance level set at $\alpha = 0.05$. Before ANOVA, the assumptions of homogeneity of variances and normality were evaluated using Bartlett's Chi-Square test and a normal plot of the raw residuals, respectively.

Results and Discussion

Bending modulus and stiffness

Figure 5 shows the results of linear regressions of the apparent bending stiffness (EI_{app}) obtained from different span bending tests for the homogeneous red oak (HRO) type of CLT glued with PRF resin. All eight types of CLT samples were similarly analyzed to obtain the regression line equations and the corresponding coefficients of determination (r^2) indicated on the graph. The average r^2 value of all 24 regressions was 0.978, ranging from 0.888 to 1.0. This average coefficient value is slightly higher than the r^2 value of 0.926 reported by Hindman and Bouldin, who used a similar multiple regression method (Hindman and Bouldin 2019).

Table 5 summarizes the flexural properties of the different types of CLT panels, based on the regression method and the shear analogy method. The coefficients of variation (COV) for the different types of CLTS ranged from 5.9 percent to 15.6 percent. This variability can be influenced by the variability in the actual Modulus of Elasticity (MOE) of the raw material, the performance of the adhesive, and the presence of local defects in the lumber. Since the CLTs were manufactured from No. 2 and No. 3 structural grade lumber, which can contain several defects such as knots, these imperfections could have a more significant impact, especially in the case of short-span bending tests. However, because of the composite structure, the CLT is less sensitive to the defects' effect than the solid timber.

In all CLT configurations, the average bending stiffness determined by tests ($EI_{eff,reg}$) exceeded the theoretical values predicted by the shear analogy method($EI_{eff,an}$). The average difference between the regression $EI_{eff,reg}$ value of the specimens and the computed $EI_{eff,an}$ from the shear analogy method was 8.9 percent, with a minimum of 4 percent and a maximum of 13.7 percent (see Table 5). The differences between the tested and predicted values in previous studies are highly inconsistent; therefore, the average difference of 8.9 percent can be considered a moderate value. For instance, Sikora et al. reported a 27 percent higher test value for three-layer CLT manufactured from 20 mm thick Irish Sitka spruce (Sikora et al. 2016). In the case of the 105 mm thick, three-layer red maple and white ash CLT, the shear analogy method underestimated the experimental apparent *EI* values by 24.1 percent and 23.9 percent, respectively (Crovella et al. 2019). On the contrary, Hematabadi et al. found that the average EI_{eff} value calculated by the regression method was 9 percent less than that obtained using the shear analogy method for three-layer CLT produced from 20 mm thick poplar lumber (Hematabadi et al. 2020). In addition to Table 5, the average bending stiffness EI_{eff} values of the specimens, categorized by method and applied adhesive, are shown in Figure 6.

As shown in Figure 6, the types of adhesives applied did not produce a statistically significant effect on the average

Table 4.—Material properties calculated from values reported by the Wood Handbook (Forest Products Laboratory, 1999).

Material	$E_L = E_1$ MPa	$E_R = E_2$ MPa	$E_T = E_3$ MPa	$G_{LR} = G_{12}$ MPa	$G_{LT} = G_{13}$ MPa	$G_{RT} = G_{23}$ MPa	$\nu_{LR} = \nu_{12}$	$\nu_{LT} = \nu_{13}$	$\nu_{RT} = \nu_{23}$
Red Oak (RO)	13,200	2,033	1,082	1,175	1,069	145*#	0.350	0.448	0.560
Red Maple (RM)	12,600	1,764	844	1,676	932	140*#	0.434	0.509	0.762
Yellow Poplar (YP)	10,900	1,003	469	818	752	130#	0.318	0.392	0.703

Notes: *Values not reported in the Wood Handbook (Forest Products Laboratory, 1999). #Avg. values calculated in Section 3.3 and reported in **Table 8** are adopted for the models.

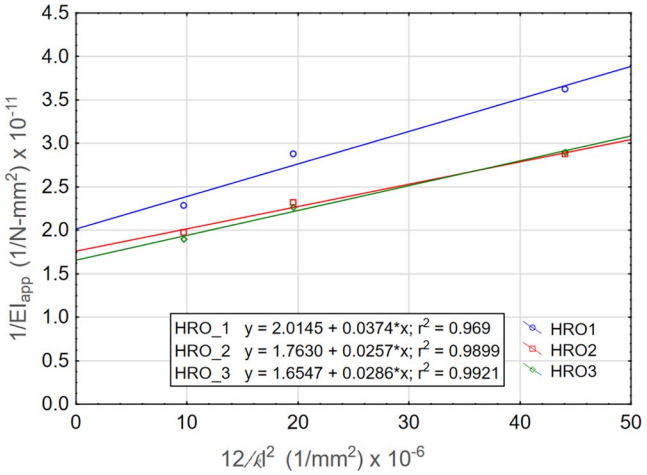

Figure 5.—Linear regression of the apparent bending stiffness and span-to-depth ratios for HRO specimens.

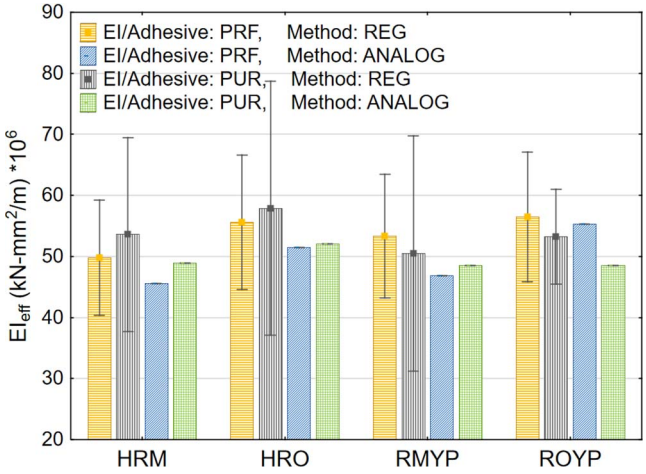

Figure 6.—Effective bending stiffness of four CLT lay-up configurations grouped by adhesive type. The whisker bars represent the standard deviation.

EI_{eff} values across all types of CLT. However, homogenous specimens (HRM and HRO) bonded with PUR resin exhibited slightly higher stiffness than those bonded with PRF resin. The average difference in the homogeneous red maple specimens was 7.6 percent, and in the homogeneous red oak samples, it was 4.1 percent. In the case of hybrid samples (RMYP and ROYP), an inverse trend was observed: PUR-bonded samples demonstrated lower average EI_{eff} values. Specifically, hybrid red maple-yellow poplar (RMYP) samples bonded with PRF showed a 5.6 percent higher average stiffness, and red oak-yellow poplar hybrids (ROYP) demonstrated a 9.1 percent increase in stiffness. Given that the variation between adhesive types remains below 10 percent, all data were consolidated into one single dataset for further analysis.

Because shear deflection plays a major role in the total deflection (bending + shear) of short-span supported CLTs, it should be calculated to ensure accurate estimates of serviceability performance (Hindman and Bouldin 2019).

Figure 7 illustrates an important change in the E_{eff}/MOE_{app} ratio across four different span-to-depth ratios for the four different lay-up configurations. The relationship between the apparent MOE and the span-to-depth ratio has been well-studied for several CLT types. However, the dependence of the E_{eff}/MOE_{app} ratio on the span-to-depth ratio has received less attention. This ratio can offer more insights into the presence of shear deflection in a given span-to-depth bending load. In general, as the span-to-depth ratio increases, the E_{eff}/MOE_{app} ratio for each type of CLT decreases, and the differences between the homogeneous and hybrid CLT also decrease. At a 30 l/d ratio, the average E_{eff}/MOE_{app} ratio was 1.09, ranging from 1.07 to 1.15, which is nearly identical to the values obtained for solid timber at an 18 l/d ratio (Nocetti et al. 2013). These findings support the conclusion that the influence of shear deformation in the CLT beam is greater than that in the solid structural timber.

Figure 8 shows the linear correlation between the apparent MOE at the 30 l/d span condition and the $E_{eff,reg}$ value from the regression model. Data from all eight types of CLT are plotted together, without distinction by type. The r^2 value of the regression line is 0.735, which is slightly lower than the $r^2 = 0.88$ reported by Nocetti et al. in the case of solid timber (Nocetti et al. 2013). However, the low p-value ($p < 0.00000$) suggests a linear correlation. Since a linear relationship exists between E_{eff} and MOE_{app}, the regression line equation can be used to calculate the effective bending stiffness (EI_{eff}) from the apparent values.

Table 5.—Flexural properties of the eight types of CLT panels.

Type of CLT	Regression analysis: Avg. $EI_{eff,reg}$ (kN-mm^2/m) *10^6	Regression analysis: Avg. $E_{eff,reg}$ (MPa) *10^3	Regression analysis: COV (%)	Shear analogy $EI_{eff,an.}$ (kN-mm^2/m) *10^6	% Diff.# $EI_{eff,reg}$ vs. $EI_{eff,an.}$
HRM-PRF	49.79	12.10	7.7	45.58	9.2
HRM-PUR	53.59	13.02	12.1	48.93	9.5
HRO-PRF	55.60	13.51	8.1	51.48	8.0
HRO-PUR	57.89	14.07	14.7	52.09	11.1
RMYP-PRF	53.31	12.96	7.7	46.87	13.7
RMYP-PUR	50.52	12.28	15.6	48.56	4.0
ROYP-PRF	58.57	14.23	6.8	55.27	5.9
ROYP-PUR	53.23	12.93	5.9	48.56	9.6

Note: # % difference = $(EI_{eff,reg} - EI_{eff,an})/EI_{eff,an}$ * 100.

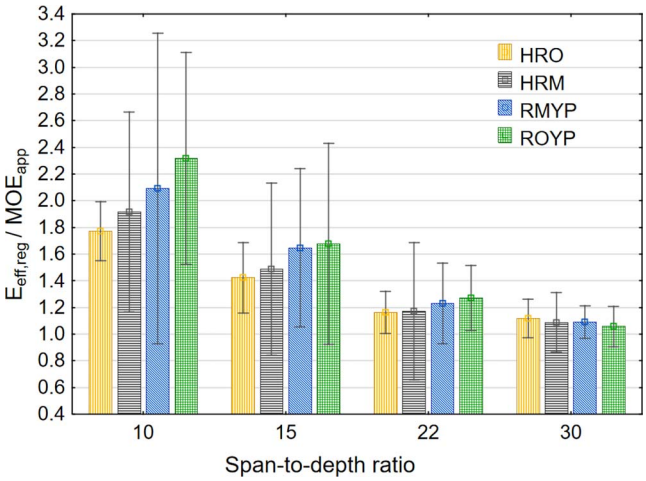

Figure 7.—E_{eff}/MOE_{app} ratios across four different span-to-depth ratios.

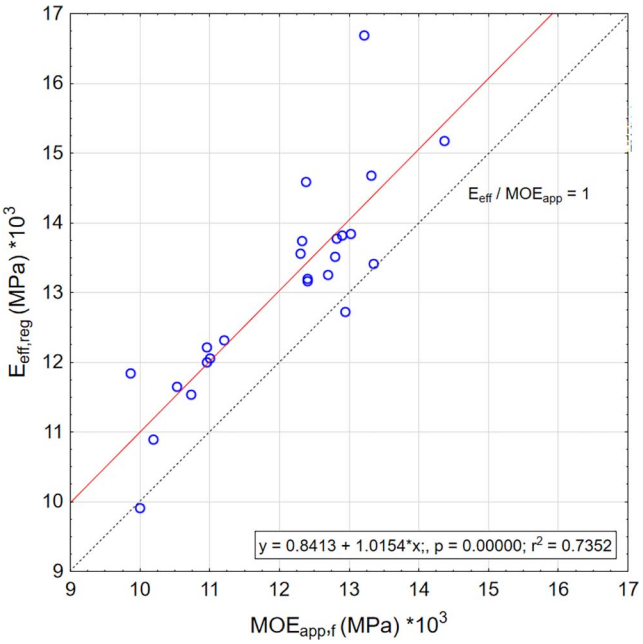

Figure 8.—Linear regression of the effective and apparent modulus of elasticity (the straight red line represents the linear regression; the dotted line represents the $E_{eff} = MOE_{app}$ line).

Effective shear stiffness

The effective shear stiffness (GA_{eff}) from the short-span bending test on CLT beams and the predicted values from the shear analogy model are shown in Table 6. The average $GA_{eff,reg}$ value ranged from 1,945 to 3,354 kN/m, depending on the CLT type, with a coefficient of variation (COV) ranging from 5.7 percent to 29.4 percent. To complement the data presented in Table 6, the average GA_{eff} values of the specimens, categorized by method and applied adhesive, are shown in Figure 9.

Except for the homogeneous CLT configurations, the specimens glued with PUR adhesive exhibited greater shear rigidity. However, no significant effect of the adhesive type was found in the measured GA_{eff} among these four types of CLT panels. The factorial ANOVA results shows that lay-ups of the CLT panels made from red maple had no influence on the GA_{eff}. For the red oak configurations, the significance level of the CLT configurations was $p < 0.05$, indicating that the lay-ups significantly affected the GA_{eff} value (Table 7).

Table 6.—Effective shear stiffness of the eight types of CLT.

Type of CLT	Sample size	Regression analysis: Avg. $GA_{eff,reg}$ (kN/m)	Regression analysis: COV %	Shear analogy $GA_{eff,an}$ (kN/m)	% Diff. $GA_{eff;\ reg}$ vs. $GA_{eff;\ an.}$
HRM-PRF	3	2,430	8.85	1,383	75.7
HRM-PUR	3	2,564	5.69	1,417	80.9
HRO-PRF	3	3,354	18.57	1,511	122.0
HRO-PUR	3	2,606	9.44	1,479	76.3
RMYP-PRF	3	2,458	8.90	1,417	73.5
RMYP-PUR	3	2,588	22.32	1,443	79.4
ROYP-PRF	3	1,945	17.74	1,449	34.2
ROYP-PUR	3	2,347	21.39	1,509	55.5

Note: % difference = $(GA_{eff,reg} - GA_{eff,an})/GA_{eff,an}$ * 100

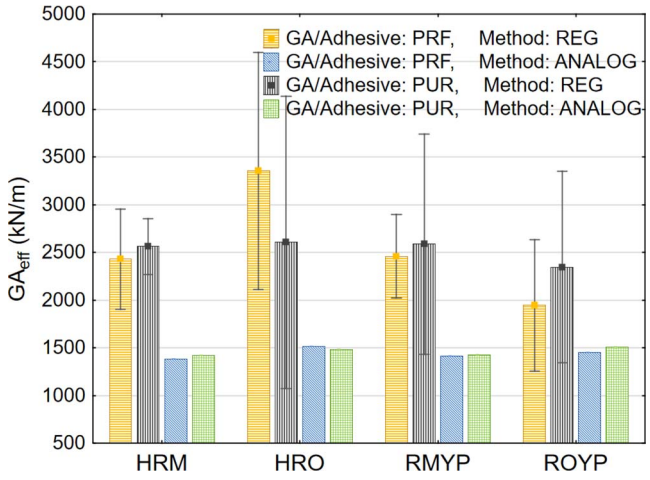

Figure 9.—Effective shear stiffness of four CLT lay-up configurations grouped by adhesive type.

Comparison of the results of the regression analyses with the predicted via Eq. 8 from the shear analogy model reveals that the analogy model underestimates the GA_{eff} value by an average of 74.8 percent. This difference is more moderate than that reported by Hematabadi et al. on poplar CLT, where the shear analogy model underestimated the effective shear stiffness by 510 percent compared with the regression method in the major strength direction (Hematabadi et al. 2020).

Shear modulus and shear strength of the short-span bending test

Detailed results of the shear tests are presented in Table 8. The average shear modulus ($G_{eff,reg}$) for the different types of CLT ranges from 108.2 MPa to 186.5 MPa, with the COV ranging from 8.9 percent to 29.44 percent. In contrast, the COV for the equivalent shear strength ($f_{s,eq}$) is narrower, ranging from 5.6 percent to 9.9 percent.

Except for the lowest average value found in the hybrid red oak glued with PRF adhesive, the shear modulus is considerably higher than that of softwood CLT, and even higher than of the homogeneous sugar maple CLT, where Ma et al. reported values of 88.67 to 97.76 MPa, depending on the adhesive used (Ma et al. 2021a).

Regardless of the CLT type, three characteristic failure modes were observed. As an example, Figure 10 shows these failures, which occurred in the #1-#6 homogeneous red oak

Table 7.—ANOVA results of the CLT samples made from red oak, which were used to evaluate the influence of various factors on the effective shear stiffness.

Effect	SS	DoF	MS	F-test	Significance level-p*
Intercept	78847440.2	1	78847440.2	233.99	*0.0000*
Adhesive type (PRF vs. PUR)	90019.9014	1	90019.9014	0.267	0.619
CLT Conf. (HOM. vs. HYB.)	2088087.67	1	2088087.67	6.196	*0.038*
Glue type* Configuration	991129.362	1	991129.362	2.941	0.124
Error	2695655.59	8	336956.948		

* Significance level of 0.05 ($p < 0.05$)

Table 8.—Shear modulus and stiffness of the eight types of CLT.

Type of CLT	Sample size	Avg. $G_{eff,reg}$ (MPa)	COV %	Avg. $f_{s,eq}$ (MPa)	COV %
HRM-PRF	3	135.2	8.85	3.28	9.87
HRM-PUR	3	142.6	5.69	3.25	6.42
HRO-PRF	3	186.5	18.57	3.13	9.24
HRO-PUR	3	144.9	29.44	3.00	9.03
RMYP-PRF	3	136.7	8.90	2.52	7.38
RMYP-PUR	3	143.9	22.32	2.50	7.85
ROYP-PRF	3	108.2	17.74	2.38	8.52
ROYP-PUR	3	130.5	21.39	2.41	5.60

(HRO) CLT specimens. The most common failure was rolling shear in the transverse layer, as observed in specimens #3 and #5. For specimens #1, #2, and #4, delamination in the adhesive layer was the second most frequent failure mode. In many cases, both failure modes appeared simultaneously (e.g., in specimen #6), suggesting that in these cases, the adhesive strength was nearly equivalent to the rolling shear strength of the wood.

The force-position curves, shown in Figure 11, also highlight the different failure patterns. In the case of rolling shear failure, multiple force peaks were observed, and the failure occurred gradually (specimens #3, and #5), whereas, in the case of pure delamination (specimens #1, #2, and #4), a significant and abrupt drop in force was noted. For specimen #6, delamination and rolling shear failure occurred together, although the force-displacement curve more closely resembled the pattern typically observed in pure delamination. Multiple shear cracks were developed through the transverse layers which propagated to the bonding line. In addition to the shear failure, tensile failure also occurred in the bottom layer, originating from a knot.

After the load–deflection across four different spans was measured to obtain the stiffness values, the strength test was carried out at a 5:1 span-to-depth ratio until failure. The equivalent shear strength ($f_{s,eq}$) values for each CLT configuration were computed via Eq. 6 and are depicted in Figure 12.

The difference in average shear strength between the homogeneous red maple CLT specimens bonded with the two different adhesives is 0.9 percent. In contrast, for the homogeneous red oak specimens, those bonded with the PRF adhesive exhibited an average shear strength 4.3 percent greater than those bonded with PUR adhesive. The strength results for the homogeneous CLT types are consistent with the findings of Crovella et al. who reported similar results for three-layer red maple ($f_s = 3.0$ MPa) and white ash ($f_s = 3.1$ MPa) CLT specimens (Crovella et al. 2019).

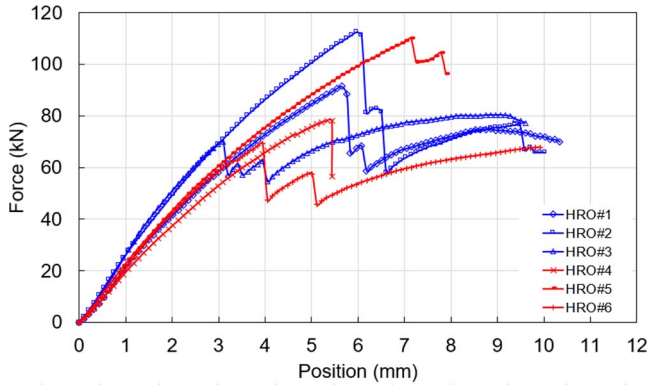

Figure 11.—Load-deflection response of homogeneous red oak (HRO) CLT specimens.

However, for both wood species, a significant difference was observed between the homogeneous and hybrid lay-up configurations. In the case of red maple, this difference averaged 30 percent, whereas for red oak, the average difference was 28 percent. This significant reduction in shear strength is attributable to the presence of the lower-strength yellow poplar. Even though the yellow poplar transverse layer reduced the shear strength of the hybrid lay-up configuration, the average shear strength of 2.51 MPa for the RMYP and 2.4 MPa for the ROYP specimens is significantly higher than that of the sugar maple–white spruce–sugar maple hybrid configuration, where Ma et al. (Ma, et al. 2021b) reported average equivalent shear strengths of 1.81 MPa and 1.7 MPa. Figure 13 shows the regression results for shear modulus and shear strength across four different CLT lay-up configurations.

Significant differences can be observed between the correlation coefficients for the four types of CLT when both types of adhesives are considered together. The strongest correlation was found for homogeneous red oak CLT ($r^2 = 0.45$), whereas a smaller correlation ($r^2 = 0.33$) was observed in homogeneous red maple CLT. Both hybrid CLTs had correlation values of $r^2 < 0.05$. Previous studies revealed that the strength of the relationship is inconsistent, as it varies by wood species. For instance Nero et al. reported similarly low correlations ($r^2 < 0.05$) for CLTs made from Eucalyptus nitens, radiata pine, and Norway spruce (Nero et al. 2022). A slightly greater correlation was observed for poplar (*Populus tremula L.*), with an r^2 of 0.08 (Ehrhart and Brandner 2018). In contrast, European beech and birch species presented significantly higher correlations, achieving r^2 values of 0.63 and 0.55, respectively (Ehrhart and Brandner 2018). None of the regressions of the four types of CLT panels have a low p-value ($p < 0.05$), indicating

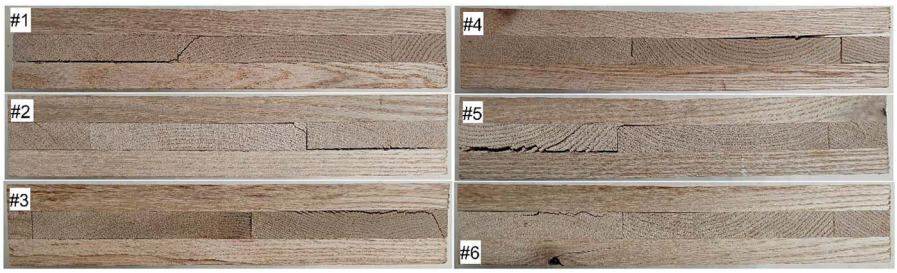

Figure 10.—Typical failure type of the short-span (5:1) shear test of the homogeneous red oak specimens (HRO), according to the ASTM D198 standard.

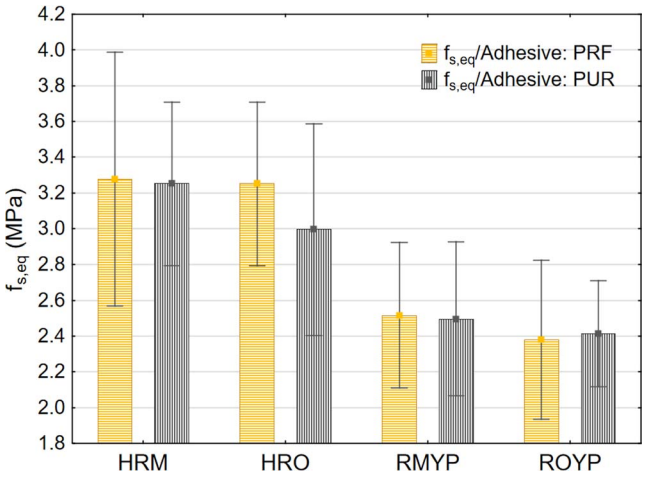

Figure 12.—Equivalent shear strength of four CLT lay-up configurations grouped by adhesive type.

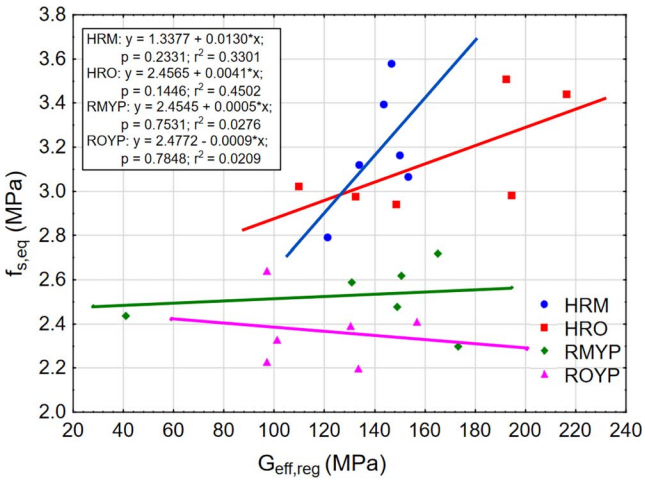

Figure 13.—Relationship between shear modulus and shear strength of four CLT lay-up configurations.

that the linear correlation between the two properties is not statistically significant. Hence, the linear equations cannot be used to estimate one property from the other.

Simulation results

Finite element (FE) models were created to explore a parallel path for the determination of the initial stiffness of CLT panels subjected to static bending tests, as described in Section 2.4, with the parameters and geometric configurations summarized in Tables 3 and 4 and Figures 2 and 3, respectively. Considering that experimental determination on elastic properties can be expensive and time-consuming, the development of FE models that can be validated with fewer experimental iterations offers a path for a broader range of design exploration and material combinations. A critical aspect of the accuracy of the FE models is the material parameters selected to reproduce the mechanical behavior of the CLT laminates. In this study, a combination of orthotropic material properties reported in the literature (Forest Products Laboratory, 1999) and shear modulus values obtained from the regression methods presented in Section 3.3 are adopted to determine the elastic response of the CLT panels subjected to center-point bending.

Figure 14 compiles deflected shapes as well as vertical displacement (U2) contours corresponding to CLT panels with spans of 574, 857, and 1245 mm subjected to prescribed displacements in the vertical direction of 2, 4, and 5 mm, respectively. Figure 14 shows the beams deform uniformly without signs of delamination or discontinuities at the bonding interfaces. Figure 15 collects the load-deflection curves observed experimentally vs. those obtained from the FE simulations for all the CLT configurations. Results compiled in Figure 15 indicate an overall good agreement between experiments and simulation results, with a slight tendency to over-predict the slope of the load-deflection curves in the ROYP and RMYP hybrid configurations, and a mix of slight under-prediction and over-prediction in the case of the HRO and HRM homogenous configurations. The slight over-prediction is attributed to the elastic cohesive properties assigned to the boding interfaces, which account for the elasticity of the bonding interface. The

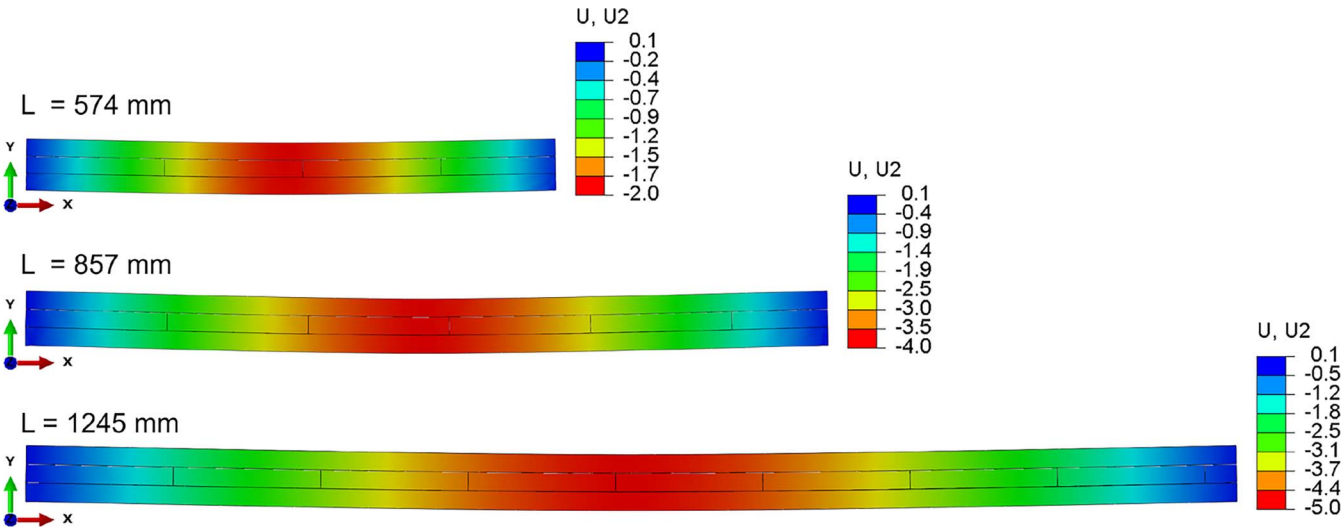

Figure 14.—Contours of vertical displacement (U2) in the global direction Y corresponding to three span lengths. Deformation amplification factor (DAF) equal to 2.

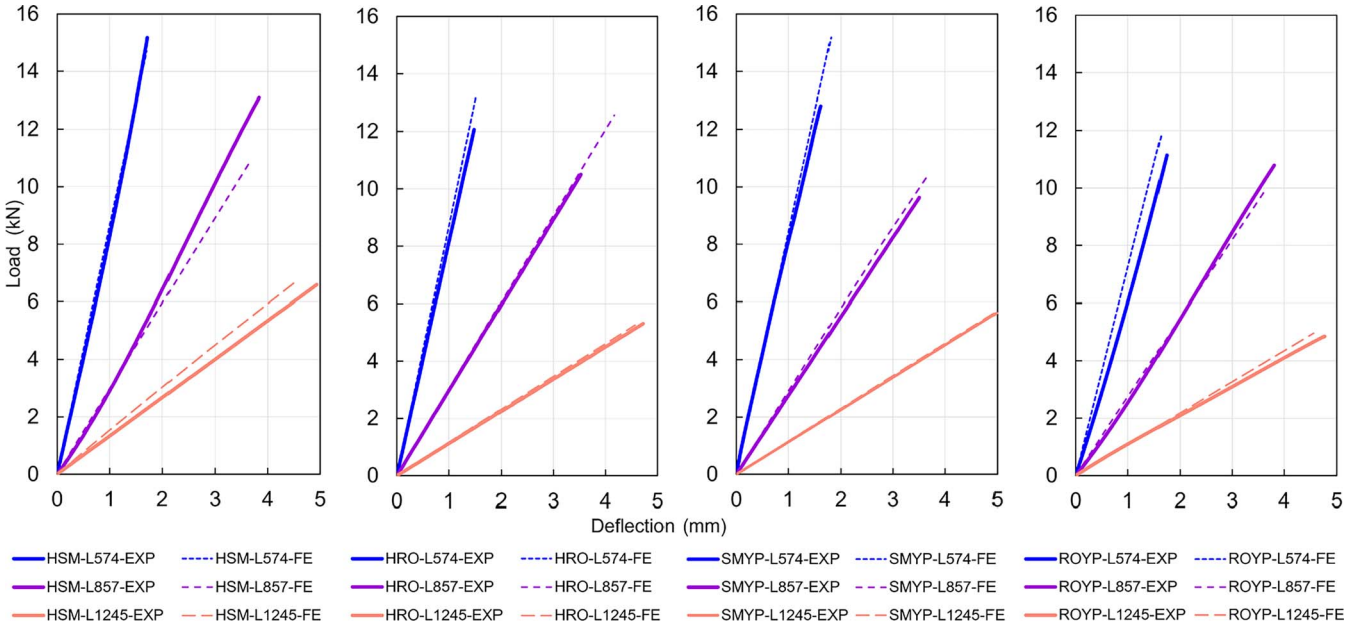

Figure 15.—Experimental (EXP) vs. Finite Element (FE) simulation load-displacement curves for all TLC configurations and three span lengths (L = 574, 857 and 1245 mm).

cohesive zone model only included cohesive elastic properties without damage initiation parameters that could capture the debonding because of failure of the adhesive, which may have started occurring in some of the experimental specimens. This simplified approach is valid for small deflections in which the strength of the adhesive is not exceeded. Further evaluations will need to be conducted to determine the damage initiation parameters corresponding to the two types of adhesives implemented in this study so the FE models can capture the potential debonding that appears beyond the linear elastic range considered in the study. Despite this limitation, the FE models created based on available material properties offer an additional way to assess the stiffness of CLTs and potentially reduce the number of experimental evaluations.

Conclusion

This study applied a variable-span regression model to assess the effective bending stiffness and shear properties of CLT made from red oak, red maple, and yellow poplar. The results highlight that the span-to-depth ratio significantly impacts the effective and apparent bending modulus ratios. However, as the span-to-depth ratio increases, the influence of shear deflection diminishes, reducing the difference between hybrid and homogeneous configurations. Whereas no substantial difference was found in the effective bending and shear stiffness between homogeneous and hybrid structures, the shear strength of hybrid configurations was 30 percent lower compared to homogeneous types. However, this value still significantly exceeds the shear strength of softwood CLT. The strong linear correlation between the apparent and effective modulus of elasticity, allows for the prediction of the effective modulus of elasticity from the apparent modulus of elasticity.

The shear analogy model consistently underestimated the shear stiffness compared to experimental results, underscoring the need for more precise predictive methods, especially for hardwood CLT. Future research should focus on refining these models and further exploring hardwood species to enhance the structural performance and market adoption of hardwood CLT.

The advantage of the hybrid combination is that it ensures the stiffness of the CLT while reducing its weight. However, in applications where significant shear forces are present, the hybrid configuration's performance is limited compared to homogeneous hardwood CLT.

Besides the mechanical tests, additional examinations are necessary to verify the bonding performance of the various CLT types under the PRG 320 standard. For this purpose, cyclic delamination tests and shear block tests will be carried out. The microscopic examination of the bond line can provide further insights into the evaluation of bonding performance, which will be part of future research. The implementation of finite element models that incorporate damage evolution parameters derived from the experimental evaluation of bonding performance will allow extending the prediction capabilities beyond the linear range presented in this study.

Acknowledgments

The research on which this article is based was partially supported by grants provided by the USDA Forest Service Wood Innovation Program (23-DG-11094200-272), the Appalachian Regional Commission (ARC), and the WVU Hardwood Research Trust (HRT) Program. The authors gratefully acknowledge Henkel North America Co. for the adhesive supply and technical assistance, and Allegheny Wood Products for the material supply.

Literature Cited

Adhikari, S., H. Quesada, and B. Bond. 2023. Design and evaluation of a shear analogy tool for custom cross-laminated timber (CLT) panels made from various wood species. *Forest Prod. J.* 73(4):293–300. https://doi.org/10.13073/FPJ-D-23-00022

Adhikari, S., H. Quesada, B. Bond, and T. Hammett. 2020. Potential of hardwood lumber in cross laminated timber in North America: A CLT

manufacturer's perspective. *Mass Timber Construction J*. 3(1):1–9. https://www.journalmtc.com/index.php/mtcj/article/view/20
Aicher, S., Z. Christian, and M. Hirsch. 2016. Rolling shear modulus and strength of beech wood laminations. *Holzforschung* 70(8):773–781. https://doi.org/10.1515/hf-2015-0229
American Panel Association (APA). 2019. ANSI/APA PRG 320: Standard for Performance-Rated Cross-Laminated Timber. The Engineered Wood Association, Tacoma, Washington. 52 pp.
American Society for Testing and Materials (ASTM). 2015. ASTM D198-15, Standard Test Methods of Static Tests of Lumber in Structural Sizes. ASTM International, Conshohocken, Pennsylvania. 23 pp.
American Society for Testing and Materials (ASTM). 2018. ASTM D2718, Standard Test Methods for Structural Panels in Planar Shear (Rolling Shear). ASTM International, Conshohocken, PA. 12 pp.
Bahmanzad, A., P. L. Clouston, S. R. Arwade, and A. C. Schreyer. 2020. Shear properties ofeastern hemlock with respect to fiber orientation for use in cross laminated timber. *J.Mater. Civ. Eng*. 32(7):04020165. https://doi.org/10.1061/(ASCE)MT.1943-5533.0003232
Bendtsen, B. A. 1976. Rolling shear characteristics of nine structural softwoods. *Forest Prod. J*. 23(11):51–56.
Brandner, R., G., Flatscher, A. Ringhofer, G. Schickhofer, and A. Thiel. 2016. Cross laminated timber (CLT): Overview and development. *Eur. J. of Wood Wood Prod.* 74(3):331–351. https://doi.org/10.1007/s00107-015-0999-5
Cherry, R., A. Manalo, W. Karunasena, and G. Stringer 2019. Out-of-grade sawn pine: A state-of-the-art review on challenges and new opportunities in cross laminated timber (CLT). *Constr. Building Mater*. 211:858–868. https://doi.org/10.1016/j.conbuildmat.2019.03.293
Crovella, P., W. Smith, and J. Bartczak. 2019. Experimental verification of shear analogy approach to predict bending stiffness for softwood and hardwood cross-laminated timber panels. *Constr. Building Mater.* 229:116895. https://doi.org/10.1016/j.conbuildmat.2019.116895
Dahl, K. B. and K. A. Malo. 2009. Linear shear properties of spruce softwood. *Wood Sci. Tech.* 43(5–6):499–525. https://doi.org/10.1007/s00226-009-0246-5
Dassault Systemes Simulia Corp. 2023. Abaqus User's Manual, Documentation Collection, Version 2023, Dassault Systemes Simulia Corp, Johnston, Rhode Island. [Computer software].
Ehrhart, T., & Brandner, R. 2018. Rolling shear: Test configurations and properties of some European soft- and hardwood species. *Eng. Structures* 172:554–572. https://doi.org/10.1016/j.engstruct.2018.05.118
Forest Products Laboratory. 1999. Wood Handbook: Wood as an engineering material. (FPL-GTR-113; p. FPL-GTR-113). USDA Forest Service, Forest Products Laboratory. https://doi.org/10.2737/FPL-GTR-113
Franke S. 2016. Mechanical Properties of Beech CLT. World Conference on Timber Engineering, Vienna Austria. https://www.researchgate.net/profile/Steffen-Franke-2/publication/312198447_MECHANICAL_PROPERTIES_OF_BEECH_CLT/links/58760b0c08ae329d6225a7a3/MECHANICAL-PROPERTIES-OF-BEECH-CLT.pdf
Gardner, C., W. G. Davids, R. Lopez-Anido, B. Herzog, R. Edgar, E. Nagy, K. Berube and S. Shaler. 2020. The effect of edge gaps on shear strength and rolling shear modulus of cross laminated timber panels. *Constr. Building Mater.* 259:119710. https://doi.org/10.1016/j.conbuildmat.2020.119710
Gong, M., D. Tu, L. Li, and Y. H. Chui. 2015. Planar shear properties of hardwood cross layer in hybrid cross laminated timber. *ISCHP* 2015:85–90.
Görlacher, R. 2002. Ein Verfahren zur Ermittlung des Rollschubmoduls von Holz. *Holz Als Roh-Und Werkstoff* 60:317–322. https://doi.org/10.1007/s00107-002-0317-x
Hassler, C., J. F. McNeel, L. Denes, J. Norris, and B. Bencsik. 2022. Challenges facing the development and market introduction of hardwood cross-laminated timbers. *Forest Prod. J*. 72(4):276–283. https://doi.org/10.13073/FPJ-D-22-00048
He, M., X. Sun, and Z. Li. 2018. Bending and compressive properties of cross-laminated timber (CLT) panels made from Canadian hemlock. *Constr. Building Mater.* 185:175–183. https://doi.org/10.1016/j.conbuildmat.2018.07.072
Hematabadi, H., M. Madhoushi, A. Khazaeyan, G. Ebrahimi, D. Hindman, and J. Loferski. 2020. Bending and shear properties of cross-laminated timber panels made of poplar (Populus alba). *Constr. Building Mater.* 265:120326. https://doi.org/10.1016/j.conbuildmat.2020.120326
Hindman, D. P. and J. C. Bouldin. 2019. Bending and shear stiffness of cross-laminated timber using a variable span bending test. *J. of Testing Eval.* 47(4): 2464–2475. https://doi.org/10.1520/JTE20160147
Huang, Z., L. Jiang, C. Ni, and Z. Chen. 2023. The appropriacy of the analytical models for calculating the shear capacity of cross-laminated timber (CLT) under out-of-plane bending. *J. Wood Sci.* 69(1):14. https://doi.org/10.1186/s10086-023-02089-y
Jakobs, A. 2005. *Zur Berechnung von Brettlagenholz mit starrem und nachgiebigem Verbund unter plattenartiger Belastung mit besonderer Berücksichtigung des Rollschubes und der Drillweichheit*. PhD thesis. Univ. der Bundeswehr, München.
Karacabeyli, E. and S. Gagnon. 2019. Canadian CLT Handbook 2019 Edition (Vol. 1). FPInnovations and Binational Softwood Lumber Council, Point-Claire, Quebec.
Li, M. 2017. Evaluating rolling shear strength properties of cross-laminated timber by short-span bending tests and modified planar shear tests. *J. Wood Sci*. 63(4): 331–337. https://doi.org/10.1007/s10086-017-1631-6
Li, M., & Ren, H. 2022. Study on the interlaminar shear properties of hybrid cross-laminated timber (HCLT) prepared with larch, poplar and OSB. *Ind. Crops Prod*., 189:115756. https://doi.org/10.1016/j.indcrop.2022.11575
Lim, H., S. Tripathi, and M. Li. 2020. Rolling shear modulus and strength of cross-laminated timber treated with micronized copper azole type C (MCA-C). *J. Wood Sci*. 259:120419. https://doi.org/10.1016/j.conbuildmat.2020.120419
Ma, Y., M. Musah, R. Si, Q. Dai, X. Xie, X. Wang, and R. J. Ross 2021a. Integrated experimental and numerical study on flexural properties of cross laminated timber made of low-value sugar maple lumber. *Constr. Building Mater*. 280:122508. https://doi.org/10.1016/j.conbuildmat.2021.122508
Ma, Y., R. Si, M. Musah, Q. Dai, X. Xie, X. Wang, and R. J. Ross 2021b. Mechanical property evaluation of hybrid mixed-species CLT panels with sugar maple and white spruce. *J. Mater. Civil Eng.* 33(7):04021171. https://doi.org/10.1061/(ASCE)MT.1943-5533.0003760
National Hardwood Lumber Association (NHLA). 2014. Rules of the Measurement and Inspection of Hardwood and Cypress. National Hardwood Lumber Association, Memphis, Tennessee.
Nero, R., P. Christopher, and T. Ngo. 2022. Investigation of rolling shear properties of cross-laminated timber (CLT) and comparison of experimental approaches. *Constr. Building Mater*. 316:125897. https://doi.org/10.1016/j.conbuildmat.2021.125897
Nocetti, M., L. Brancheriau, M. Bacher, M. Brunetti, and A. Crivellaro. 2013. Relationship between local and global modulus of elasticity in bending and its consequence on structural timber grading. *Eur. J. Wood Wood Prod*. 71(3):297–308. https://doi.org/10.1007/s00107-013-0682-7
Northeastern Lumber Manufacturers Association (NELMA). 2024 Standard Grading Rules for Northeastern Lumber. Northeastern Lumber Manufacturers Association, Cumberland Center Maine. https://nelma.org/wp-content/uploads/2021/10/Section0_TOC_GRB2021.pdf
Rahman, M., M. Ashraf, K. Ghabraie, and M. Subhani. 2020a. Evaluating Timoshenko method for analyzing CLT under out-of-plane loading. *Buildings* 10(10):184. https://doi.org/10.3390/buildings10100184
Rahman, M., M. Ashraf, K. Ghabraie, and M. Subhani. 2020b. Assessment of shear analogy and Timoshenko method for analyzing hybrid CLT under out-of-plane loading. *Proc. Int. Structural Eng. and Construction* 7(2):2020. https://doi.org/10.14455/ISEC.2020.7(2).MAT-17 MAT-17-1–MAT-17-3
Rara A.D.S. 2021. Rolling shear strength and modulus for various southeastern US wood species using the two-plate shear test. *Virginia Tech*. http://hdl.handle.net/10919/104017
Sandoli, A. and B. Calderoni. 2020. The rolling shear influence on the out-of-plane behavior of CLT panels: A comparative analysis. *Buildings* 10(3):42. https://doi.org/10.3390/buildings10030042
Schultz, J. 2017. Comparison of CLT design methods to composite beam theory. 39th IABSE Symposium-Engineering the Future, September 21–23, 2017, Vancouver, Canada. https://www.researchgate.net/profile/Joshua-Schultz/publication/349193886_Comparison_of_CLT_Design_Methods_to_Composite_Beam_Theory/links/61c22701c99c4b37eb12d6a7/Comparison-of-CLT-Design-Methods-to-Composite-Beam-Theory.pdf
Sikora, K. S., D. O. McPolin, and A. M. Harte 2016. Effects of the thickness of cross-laminated timber (CLT) panels made from Irish Sitka spruce on

mechanical performance in bending and shear. *Constr. Building Mater.* 116:141–150. https://doi.org/10.1016/j.conbuildmat.2016.04.145

Tran, V.-D., M. Oudjene, and P.-J. Méausoone. 2014. FE analysis and geometrical optimization of timber beech finger-joint under bending test. *Int. J. Adhes. and Adhes*. 52:40–47. https://doi.org/10.1016/j.ijadhadh.2014.03.007

Tran, V.-D., M. Oudjene, and P.-J. Méausoone. 2015. Experimental and numerical analyses of the structural response of adhesively reconstituted beech timber beams. *Compos. Structures* 119:206–217. https://doi.org/10.1016/j.compstruct.2014.08.013

Wang, J., T. Han, Q. Lv, Y. Liu, S. Zhao, and S. Yang. 2024. Rolling shear properties of cross-laminated bamboo (CLB) specimens: A comprehensive study. *Constr. Building Mater.* 414:135052. https://doi.org/10.1016/j.conbuildmat.2024.135052

Wang, Z., H. Fu, M. Gong, J. Luo, W. Dong, T. Wang, and Y. H. Chui. 2017. Planar shear and bending properties of hybrid CLT fabricated with lumber and LVL. *Constr. Building Mater.* 151:172–177. https://doi.org/10.1016/j.conbuildmat.2017.04.205

Wang, Z., M. Gong, and Y.-H. Chui. 2015. Mechanical properties of laminated strand lumber and hybrid cross-laminated timber. *Constr. Building Mater*. 101:622–627. https://doi.org/10.1016/j.conbuildmat.2015.10.035

Wang, Z., J. Zhou, W. Dong, Y. Yao, and M. Gong. 2018. Influence of technical characteristics on the rolling shear properties of cross laminated timber by modified planar shear tests. *Maderas, Cienc. Tecnol.* 20(3). http://dx.doi.org/10.4067/S0718-221X2018005031601

Yang, S., H. Lee, G. Choi, and S. Kang. 2023. Mechanical properties of hybrid cross-laminated timber with wood-based materials. *Ind. Crops and Prod*. 206:117629. https://doi.org/10.1016/j.indcrop.2023.117629

Zhou, Q., M. Gong, Y. H. Chui, and M. Mohammad. 2014. Measurement of rolling shear modulus and strength of cross laminated timber fabricated with black spruce. *Constr. Building Mater*. 64:379–386. https://doi.org/10.1016/j.conbuildmat.2014.04.039